

# Effect of process parameters on induction plasma reactive deposition of tungsten carbide from tungsten metal powder<sup>①</sup>

JIANG Xian-liang(蒋显亮)<sup>1</sup>, M. I. Boulos<sup>2</sup>

(1. Institute of Surface and Coatings Technology, Central South University, Changsha 410083, P. R. China;

2. Department of Chemical Engineering, University of Sherbrooke, Sherbrooke, J1K 2R1, Canada)

**[Abstract]** Tungsten carbide deposit was made directly from tungsten metal powder through the reaction with methane in radio frequency induction plasma. Effect of major process parameters on the induction plasma reactive deposition of tungsten carbide was studied by optical microscopy, scanning electron microscopy, X-ray diffraction analysis, water displacement method, and microhardness test. The results show that methane flow rate, powder feed rate, particle size, reaction chamber pressure and deposition distance have significant influences on the phase composition, density, and microhardness of the deposit. Extra carbon is necessary to ensure the complete conversion of tungsten metal into the carbide.

**[Key words]** induction plasma; tungsten carbide; deposit; carburization; phase composition

**[CLC number]** TG 156.8

**[Document code]** A

## 1 INTRODUCTION

Tungsten carbide is widely used as cutting tool insert and wear-resistant coating material because of its high hardness and good thermal shock resistance. Traditionally, tungsten carbide is produced through the carburization reaction between tungsten metal and carbon at high temperature for a long time. Large grain growth during the long time carburization process results in low mechanical properties of subsequent sintering products.

In 1992, Smith<sup>[1,2]</sup> reported that WC and TiC particles were formed in d. c. plasma, via the reaction of W and Ti metal powders with methane. Due to the small volume of d. c. plasma, short particle residence time, and lateral injection of powder, only a fraction of the injected powders were carburized. As a result, WC/W and TiC/Ti composites with low deposit densities were made. JIANG et al. reported<sup>[3]</sup> that the deposits of tungsten and titanium carbides were made through the reaction of tungsten and titanium metal powders with methane in induction plasma. Formation of the carbides was completed by first carburization of the metal powders in the reactive plasma and by further carburization of the deposits on substrate at high temperature<sup>[4]</sup>.

In the past decade, induction plasma was evolved as a new technology applied in the melting, spheroidization and deposition of large particle size refractory materials like W, Mo and Al<sub>2</sub>O<sub>3</sub><sup>[5~7]</sup>, processing of ceramic TiC<sup>[8]</sup>, synthesis of ultrafine SiC<sup>[9]</sup> and Si<sub>3</sub>N<sub>4</sub><sup>[10]</sup>, spray-forming of hydroxyapatite via suspension injection<sup>[11]</sup>, fabrication of solid oxide

fuel cells<sup>[12]</sup>, and destruction of toxic waste<sup>[13]</sup>. All these applications of the inductively coupled radio frequency plasma are attributed to the favorite characteristics of the induction plasma including large plasma volume, long particle residence time, central powder feeding, and lack of electrode<sup>[14]</sup>.

This study emphasizes on the process of the reactive plasma deposition and the effect of major process parameters on the phase composition, density, and microhardness of the deposit.

## 2 EXPERIMENTAL

The reactive plasma deposition of tungsten carbide from tungsten metal powder was conducted in a large chamber that was connected to a rotary pump. A schematic of the experimental set-up is shown in Fig. 1. Frequency used for the generation of the plasma was 3 MHz. The highest applicable plasma power was 50 kW. Ar gas was used as central plasma gas and Ar+ H<sub>2</sub> mixture as sheath plasma gas. Flow rates of these gases are given in Table 1.

To obtain the deposit, a 100 mm graphite substrate was placed at the upper position of the chamber. The graphite substrate was sprayed with BN aerosol to facilitate removal of the deposit from the substrate after cooling. Measurement of substrate temperature was made by a pyrometer. The measurement was conducted immediately after the extinction of the plasma at the end of deposition.

Major process parameters studied are methane flow rate, powder feed rate, tungsten particle size, reaction chamber pressure, and deposition distance. Ranges of these variables are also shown in Table 1.

**Table 1** Induction plasma reactive deposition conditions

Process parameters	Values
Central plasma gas flow rate	40 L/min (Ar)
Sheath plasma gas flow rate	90 L/min (Ar) + 9 L/min (H <sub>2</sub> )
Plasma power	50 kW
Methane flow rate	2~17 L/min
Tungsten powder feed rate	10~30 g/min
Tungsten particle size	5~75 μm
Chamber pressure	27~53 kPa
Deposition distance	200~450 mm

Dependable variables studied are phase composition that was analyzed by X-ray diffraction, deposit density that was measured by water displacement method, and microhardness that was tested under the load of 300 g. SEM was used for examination of tungsten metal powder and top surface of the deposit, and optical microscopy for examination of the cross section of the deposit.

### 3 RESULTS AND DISCUSSION

#### 3.1 Reactive plasma deposition

Morphology of tungsten metal powder is shown in Fig. 2. It is seen from the SEM micrograph that the powder consists of polynomial particles and particle clusters. Mean particle size of the powder is approximately 5 μm. The powder was axially injected into the plasma with a carrier gas. In the induction plasma, tungsten particles reacted with the species decomposed from methane, forming deposits on the graphite substrate. Microstructure at the central area of a representative deposit is shown in Fig. 3. The de-

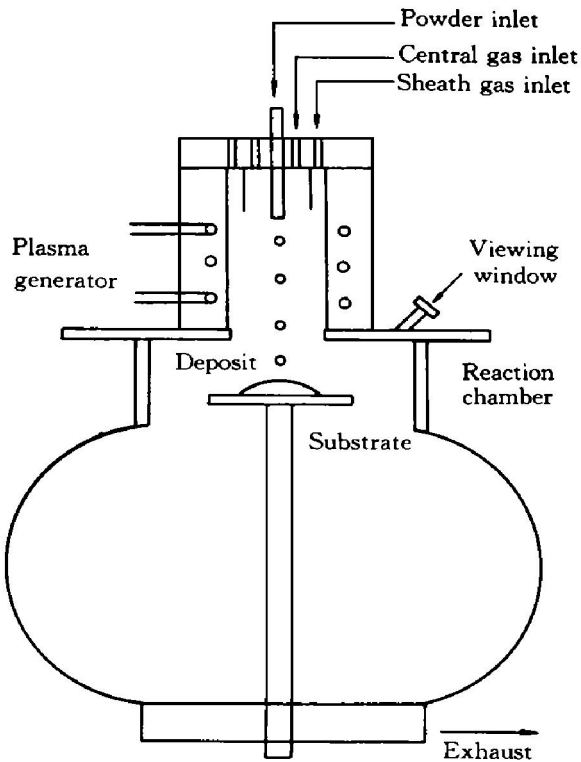


**Fig. 1** Schematic of experimental set-up used for induction plasma reactive deposition

posit is made under the condition of plasma power level of 50 kW, methane flow rate of 4.2 L/min, powder feed rate of 10 g/min, particle size of 5 μm, reaction chamber pressure of 27 kPa, and deposition distance of 200 mm. Small grains with a size of about 3 μm are illustrated in this figure. No laminar layer or crack is found in this deposit. X-ray diffraction pattern from the central area of this deposit is presented in Fig. 4(a). Major phase at the central

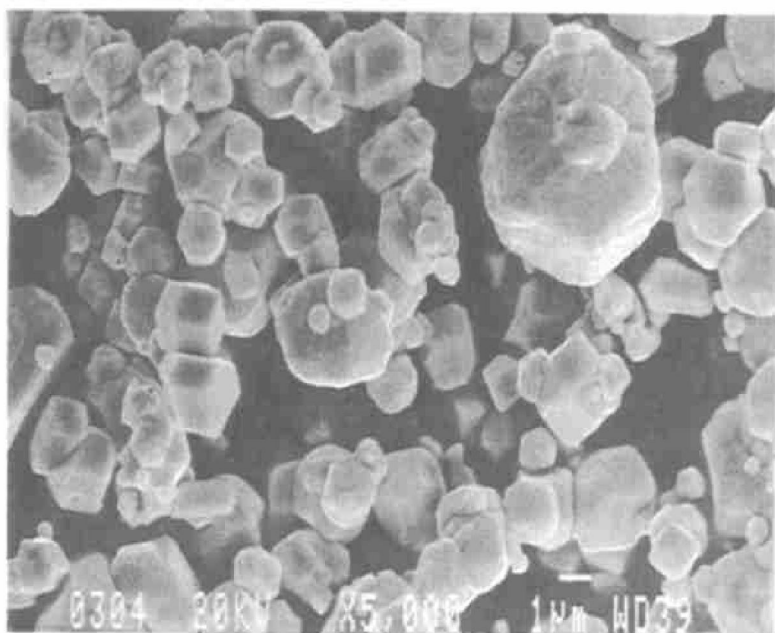


**Fig. 2** SEM micrograph of starting tungsten powder

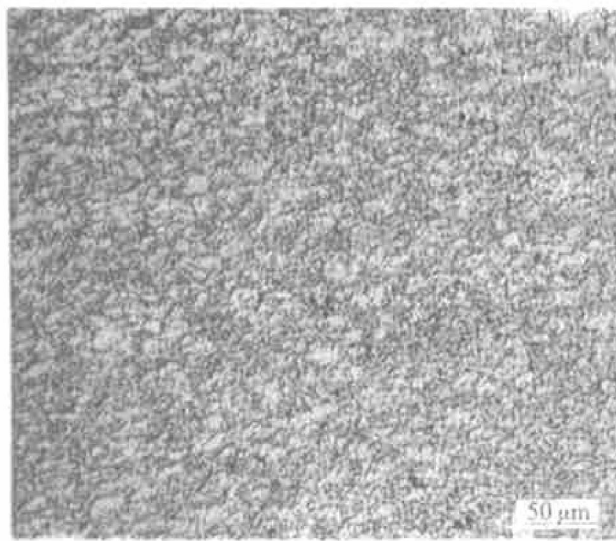


**Fig. 3** Optical micrograph of middle cross section of representative tungsten carbide deposit made from tungsten metal under typical plasma spray condition

area is  $W_2C$ . No tungsten metal is found. The phase composition, density and microhardness of this deposit are shown in Table 2. Density of this deposit is  $16.0\text{ g/cm}^3$ , equivalent to 4% porosity, taken into account of the phase composition of 9%  $WC + 91\% W_2C$  (mass fraction). Microhardness at the central area of this deposit is  $Hv2044$ .

It should be pointed out that there are some variations in the porosity, phase composition, and microhardness of the deposit from the bottom to the top. Porosity of the deposit is higher at the top than at the bottom, a typical phenomenon occurred during plasma spray forming of deposit with a conical shape. The content of  $WC$  phase at the bottom of the deposit is higher because there is more time at the bottom than at the top for carbon to diffuse into tungsten and/or form tungsten carbide ( $W_2C$ ) during the further carburization of the deposit on the substrate at high temperature. The higher density and the higher  $WC$  content result in the higher microhardness ( $Hv2170$ ) at the bottom of the deposit.

### 3.2 Influence of methane flow rate

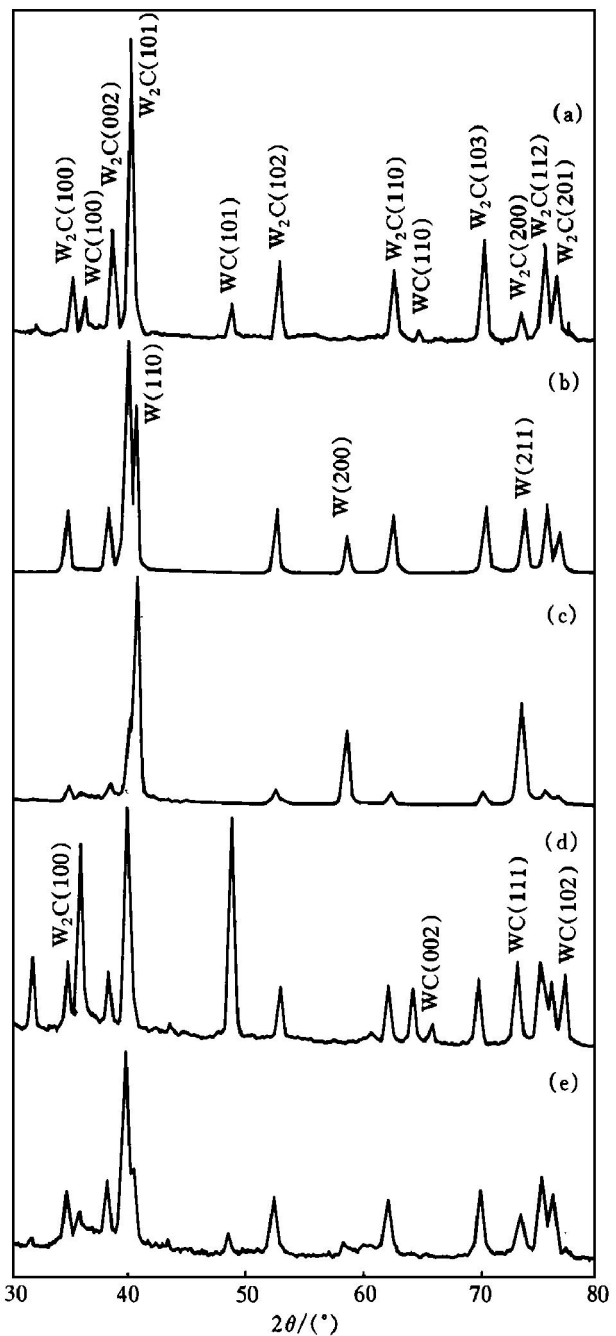


**Fig. 4** XRD patterns of middle cross sections of deposits made from tungsten powder under different reactive plasma spray conditions  
 (a) —Condition 1; (b) —Condition 3; (c) —Condition 4;  
 (d) —Condition 5; (e) —Condition 6

**Table 2** Effect of major process parameters on phase composition, porosity, and microhardness of deposit

Condition	Methane flow rate / ( $\text{L} \cdot \text{min}^{-1}$ )	Powder feed rate / ( $\text{g} \cdot \text{min}^{-1}$ )	Particle size/ $\mu\text{m}$	Chamber pressure/ kPa	Deposition distance/ mm	Phase composition (mass fraction, %)	Porosity / %	$Hv(300)$
1	4.2	10	5	27	200	9WC + 91 $W_2C$	4	2 044
2	2.0	10	5	27	200	6WC + 87 $W_2C$ + 7W	4	1 887
3	4.2	30	5	27	200	65 $W_2C$ + 35W	5	1 668
4	4.2	10	45~75	27	200	20WC + 80W	3	707
5	4.2	10	5	53	200	37WC + 63 $W_2C$	8	1 050
6	4.2	10	5	27	300	5WC + 79 $W_2C$ + 16W	6	1 439

The influence of methane flow rate on the phase composition, density/ porosity, and microhardness of the deposit can be found in Table 2. Methane flow rate of 4.2 L/min and tungsten powder feed rate of 10 g/min were used for making the deposit, corresponding to  $x(C)/x(W)$  ratio of 3.5 (mole ratio of carbon in methane to tungsten). When methane flow rate was reduced to 2.0 L/min, the  $x(C)/x(W)$  ratio was changed to 1.7. At this time, the contents of WC and  $W_2C$  in the deposit decrease while the content of W increases. It is understood that it is not all carbon atoms to react with tungsten during the reactive plasma deposition because a lot of carbon are extracted out of plasma and attached on the wall of the reaction chamber. On the ground of the experimental result, it is required that the  $x(C)/x(W)$  ratio must be much greater than 1.0 to make the carburization of tungsten complete.

Nevertheless, this doesn't mean that the higher the methane flow rate, the better the carburization process, because extra carbon involved into the deposit can cause the decline of deposit density or even can not lead to the formation of the deposit on the substrate.

When methane flow rate was reduced from 4.2 L/min to 2.0 L/min, porosity of 4% in the deposit did not change, as indicated in Table 2, but microhardness decreased from Hv2044 to Hv1887 as a result of the reduction of WC phase.

### 3.3 Influence of powder feed rate

When powder feed rate was increased from 10 g/min to 30 g/min while methane flow rate was unchanged, the  $x(C)/x(W)$  ratio decreases to about 1.2. At this time, WC phase is not presented in the X-ray diffraction pattern of the deposit, as shown in Fig. 4(b). Moreover, a fraction of tungsten metal is not carburized.  $W_2C$  phase content declined from 91% to 65% (mass fraction). Obviously, the methane flow rate at the  $x(C)/x(W)$  ratio of 1.2 is not sufficient to make the carburization of tungsten metal complete. The remarkable reduction of the carbide in the deposit gives rise to the large decline of microhardness, as shown in Table 2. Similar to the deposition of tungsten metal in induction plasma, the high powder feed rate results in small increase of porosity in the deposit.

### 3.4 Influence of particle size

It is shown in Fig. 4(c) that the influence of particle size on the phase composition of the deposit is significant. Due to the limit of tungsten powder sources, only the coarse powder with a particle size of 45~75  $\mu\text{m}$  was used. Phase composition of a representative deposit made from this coarse powder is 20%  $W_2C$ + 80% W (mass fraction). No WC phase is found in this deposit. Because large size powder has a

small specific surface area, the conversion of tungsten metal into carbide through surface diffusion in the reactive plasma is slowed down. The distance of carbon diffusion into the center increases. Moreover, the involvement of carbon into the deposit mainly through carbon attachment on particle surface decreases. All these factors lead to the reduction of the carbide formed in the deposit.

As large size tungsten powder is melted in the reactive plasma, the relative density of the deposit reaches 97%. Because of the small amount of tungsten carbide form in the deposit, microhardness of this deposit is only Hv707, but still higher than the microhardness (Hv427) of tungsten metal deposit with same apparent density.

### 3.5 Influence of chamber pressure

Because the reactive plasma deposition is conducted under reduced pressures, the variation of chamber pressure can change the properties of the deposit. As shown in Fig. 4(d) and Table 2, the content of WC phase in the deposit remarkably increased from 9% to 37% (mass fraction) when the pressure of the reaction chamber was raised from 27 kPa to 53 kPa. This experimental phenomenon is explained as follows. Firstly, according to thermodynamic theory, the reaction of tungsten particles with the species of methane is faster at a higher pressure. More tungsten is converted into  $W_2C$  or even WC in the reactive plasma. Secondly, at a higher chamber pressure, less carbon is extracted out of the plasma and more carbon is evolved into the deposit. As a result, more  $W_2C$  is converted into WC on the substrate at high temperature. When chamber pressure was raised from 27 kPa to 53 kPa, however, porosity in the deposit went up from 4% to 8%. Consequently, the contribution from the increased WC phase in the deposit to the gain of microhardness is insufficient to compensate the loss of microhardness caused by the decreased density. It is implied that deposit density has a greater effect on microhardness than carbide content in the deposit has.

### 3.6 Influence of deposition distance

Deposition distance is the length between the exit of the powder injector and the substrate. When deposition distance was increased from 200 mm to 300 mm, contents of WC and  $W_2C$  phases in the deposit decreased while that of W phase increased, as shown in Fig. 4(e) and Table 2. It is known that the enhancement of the carburization of tungsten in the plasma through the increase of particle residence time at a large spray distance is extremely limited because the total particle residence time in induction plasma is less than 100 ms. At the increased deposition distance, the involvement of carbon into the deposit gets less and substrate temperature becomes lower. The

combined effect of less carbon involvement and lower substrate temperature remarkably reduces the formation of the tungsten carbide on the substrate. It can be inferred that the contribution from the further carburization on the substrate to the formation of the carbide exceeds that from the first carburization in the reactive plasma.

Since the melting point of tungsten is 3410 °C, the long deposition distance of 300 mm caused some particles solidify before reaching on the substrate, resulted in the decrease of deposit density. The reduced carbide content in the deposit and the decreased density make microhardness decline from Hv2044 to Hv1439.

#### 4 CONCLUSIONS

1) Major process parameters such as methane flow rate, tungsten powder feed rate, particle size, chamber pressure, and deposition distance have significant effects on the phase composition, porosity, and microhardness of tungsten carbide formed during the reactive plasma deposition. Variation of either carbide content or porosity in the deposit causes the change of microhardness.

2) Extra carbon is necessary to ensure the complete conversion of tungsten metal into the carbide.

3) Contribution from further carburization of the deposit on substrate at high temperature to the formation of tungsten carbide exceeds that from the first carburization of tungsten powder in the reactive plasma.

#### [ REFERENCES]

- [1] Smith R W, Mutazim Z Z. Reactive plasma spraying of wear-resistant coating [J]. *Journal of Thermal Spray Technology*, 1992, 1: 57– 63.
- [2] Smith R W. Reactive plasma spray forming for advanced materials synthesis [J]. *Powder Metallurgy International*, 1993, 25: 9– 16.

- [3] Jiang X L, Tiwari R, Gitzhofer F, et al. Induction plasma reactive deposition of tungsten and titanium carbides [A]. 7th National Thermal Spray Conf. [C]. USA: Boston, 1994. 451– 456.
- [4] Jiang X L, Tiwari R, Gitzhofer F, et al. Reactive plasma deposition of tungsten and titanium carbides by induction plasma [J]. *Journal of Materials Science*, 1995, 30: 2325– 2329.
- [5] Jiang X L, Tiwari R, Gitzhofer F, et al. On the induction plasma deposition of tungsten metal [J]. *Journal of Thermal Spray Technology*, 1993, 2: 265– 270.
- [6] Jiang X L, Fan X B, Gitzhofer F, et al. Induction plasma spraying of refractory materials [A]. 13th Inter Thermal Spray Conf [C]. USA: Orlando, 1992. 39– 44.
- [7] Fan X B, Gitzhofer F, Boulos M I. Statistical design of experiments for the spheroidization of powdered alumina by induction plasma processing [J]. *Journal of Thermal Spray Technology*, 1998, 7: 247– 253.
- [8] Ishigaki T, Jurewicz J, Tanaka J, et al. Compositional modification of titanium carbide powders by induction plasma treatment [J]. *Journal of Materials Science*, 1995, 30: 883– 890.
- [9] Guo J Y, Gitzhofer F, Boulos M I. Induction plasma synthesis of ultrafine SiC powder from silicon and CH<sub>4</sub> [J]. *Journal of Materials Science*, 1995, 30: 5589– 5599.
- [10] Soucy G, Jurewicz J, Boulos M I. Parametric study of the thermal plasma synthesis of ultrafine silicon nitride powder [J]. *Journal of Materials Science*, 1995, 30: 2008– 2018.
- [11] Bouyer E, Gitzhofer F, Boulos M I. The suspension plasma spraying of bioceramics by induction plasma [J]. *JOM*, 1997, 2: 58– 62.
- [12] Henne R, Muller M, Pross E, et al. Near-net-shape forming of metallic bipolar plates for planar solid oxide fuel cells by induction plasma spraying [J]. *Journal of Thermal Spray Technology*, 1999, 8: 110– 116.
- [13] Yargeau V, Soucy G, Boulos M I. The treatment of a water-based toxic waste using induction plasma technology [J]. *Plasma Chemistry and Plasma Processes*, 1999, 19: 327– 340.
- [14] Boulos M I. The inductively coupled radio frequency plasma [J]. *Journal of High Temperature Material Process*, 1997, 1: 17– 39.

(Edited by YANG Bing)